

Dual-Band Dual-Polarized Antenna Design for Polarization-Insensitive Up-link Power Transmission and Down-link Harmonic Backscatters

Hao Zhang ⁽¹⁾

(1) School of Microelectronics, Northwestern Polytechnical University; e-mail: zhang.hao@nwpu.edu.cn

Abstract

To qualify requirements of polarization-insensitive up-link power transmission and down-link harmonic backscatters, dual-band dual-polarized antenna was designed, fabricated and measured, which achieves excellent gains of radiation patterns and isolation between horizontal (HP) and vertical (VP) polarizations within dual bands of ω_0 and $2\omega_0$ ($\omega_0 = 2.45$ GHz) by sharing identical physical antenna aperture.

1 Introduction

Wireless power transmission demonstrates an effective and robust solution to extend lifespan of micro unmanned aerial vehicles (micro-UAVs) [1, 2]. However, it always suffers misalignment of maximum radiation patterns as illustrated by Fig. 1, which seriously degrades wireless link efficiency between the transmitting (TX) and receiving (RX) antennas.

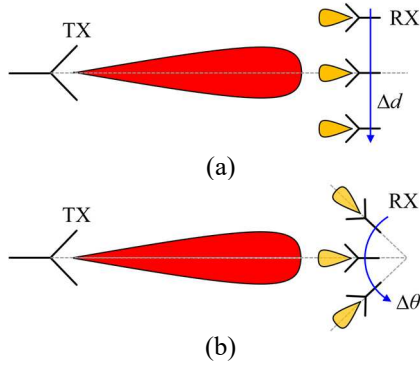


Figure 1. Misalignment of the maximum radiation patterns between TX and RX antennas with (a) distance, Δd and (b) angle, $\Delta\theta$ variations.

To align maximum radiation patterns, harmonics generated from nonlinearity of rectifiers (i.e., Schottky diodes) can be exploited [3, 4]. In Fig. 2, polarization-insensitive up-link power transmission and down-link harmonic backscatters is proposed, which establishes dual high-isolation channels insensitive to antenna polarization tilt, φ with an integration of dual-band (ω_0 and $n\omega_0$) hybrid couplers [5, 6] and dual-band dual-polarized antennas positioned symmetrically. In this research, operation mechanism of schematic from Fig. 2 is primarily analysed and then detailed procedures of the dual-band dual-polarized antenna design is provided.

This paper's copyright is held by the author(s). It is published in these proceedings and included in any archive such as IEEE Xplore under the license granted by the "Agreement Granting URSI and IEICE Rights Related to Publication of Scholarly Work."

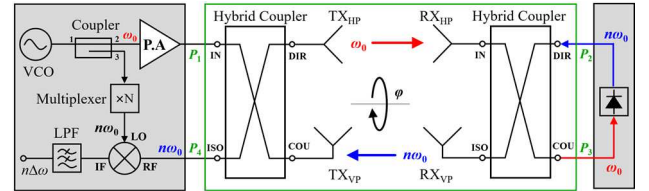


Figure 2. Schematic of the polarization-insensitive up-link power transmission and down-link harmonic backscatters.

2 High-Isolation Channels Establishment

Fig. 2 indicates that a four-port network (P_1, P_2, P_3, P_4) can be cascaded with dual-band hybrid couplers, TX and RX dual-band dual-polarized antennas. The polarization tilt, φ varied from 0° to 360° between TX and RX antennas can be depicted with Fig. 3.

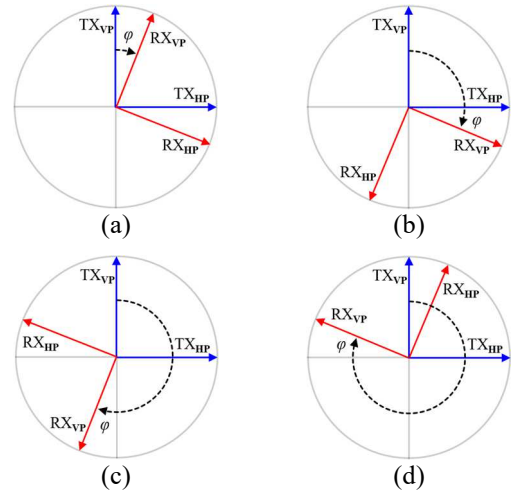


Figure 3. Varied angles of the polarization tilt (a) $0^\circ < \varphi < 90^\circ$, (b) $90^\circ < \varphi < 180^\circ$, (c) $180^\circ < \varphi < 270^\circ$, (d) $270^\circ < \varphi < 360^\circ$.

The normalized four-port S-parameters between dual-band dual-polarized antennas, $[S]$ can be derived from Fig. 3.

$$[S] = \begin{bmatrix} 0 & \cos \varphi & -\sin \varphi & 0 \\ \cos \varphi & 0 & 0 & \sin \varphi \\ -\sin \varphi & 0 & 0 & \cos \varphi \\ 0 & \sin \varphi & \cos \varphi & 0 \end{bmatrix} \quad (1)$$

Hence, S-parameters of the four-port network (i.e., green box: P_1, P_2, P_3, P_4) from Fig. 2 are calculated as follows.

$$[S] = \begin{bmatrix} 0 & 0 & i \cos \varphi & 0 \\ 0 & 0 & -\sin \varphi & 0 \\ i \cos \varphi & 0 & 0 & i \cos \varphi \\ -\sin \varphi & 0 & 0 & +\sin \varphi \\ 0 & i \cos \varphi & 0 & 0 \\ 0 & +\sin \varphi & 0 & 0 \end{bmatrix} \quad (2)$$

It demonstrates that the magnitudes of $S''_{31}=i\cos\varphi+\sin\varphi$ and $S''_{42}=i\cos\varphi+\sin\varphi$ behave constant regardless of polarization tilt, φ within dual bands of ω_0 and $n\omega_0$. Hence, dual high-isolation channels are established and validated for up-link power transmission and down-link harmonic backscatters.

3 Dual-Band Dual-Polarized Antenna ($n=2$)

As illustrated by Fig. 4, a dual-band dual-polarized antenna is evolved from the conventional patch antenna. Edges of the square patch contribute to fundamental frequency band, and second harmonic frequency band resonances are driven by probes. To achieve directional radiations, four slots are etched on the patch.

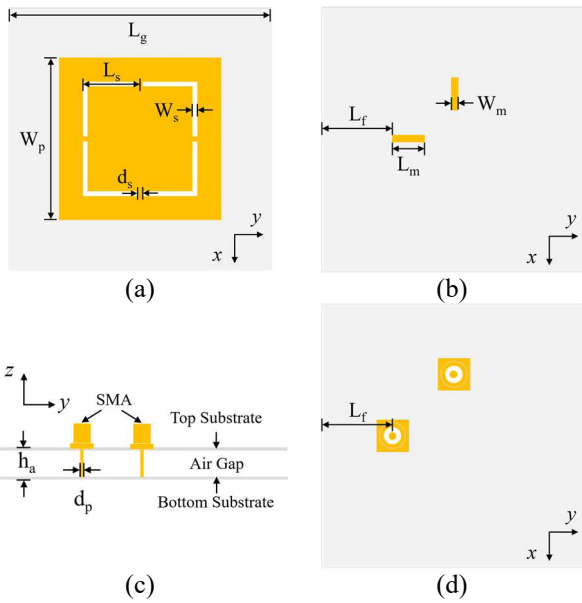


Figure 4. (a) Top and (b) bottom layers of the top substrate. (c) Side view. (d) Bottom layer of the bottom substrate.

The antenna is designed and optimized by CST studio suite software on a 20-mil low-loss substrate, Rogers RO4350B ($\epsilon_r = 3.66$, $\tan \delta = 0.0037$) at dual bands of $\omega_0 = 2.45$ GHz and $2\omega_0 = 4.90$ GHz. The simulation and measurement of S-parameters are provided by Fig. 5(a), which achieves $|S_{11}| < -10$ dB and $|S_{21}| < -20$ dB within bandwidths from 2.38 to 2.48 GHz and 4.71 to 5.1 GHz, simultaneously. On account of geometrical symmetry of the antenna, only its radiation patterns at the VP direction are demonstrated by Fig. 5(b), whose maximum gains of E-plane and H-plane radiation patterns at 2.45 GHz and 4.90 GHz are provided with high isolation between co-/cross-polarization.

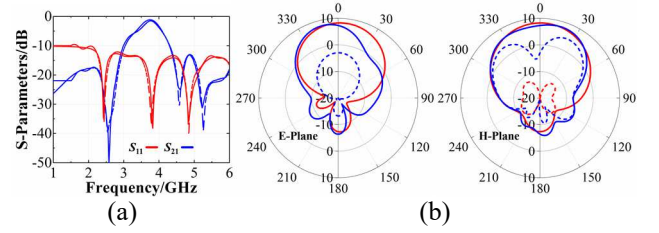


Figure 5. (a) S-parameters, and (b) radiation patterns of the dual-band dual-polarized antenna.

4 Conclusion

In this research, scheme of polarization-insensitive up-link power transmission and down-link harmonic backscatters is proposed and theoretically analyzed. Meanwhile, a dual-band dual-polarized antenna was designed, fabricated and measured, which attains excellent performance of radiation pattern and polarization isolation for such proposed scheme.

Acknowledgements

This research was supported in part by the National Natural Science Foundation of China (62001395), Natural Science Basic Research Program of Shaanxi (2021JQ-125), Basic Research Programs of Taicang (TC2020JC12).

References

- [1] B. Strassner and K. Chang, "Microwave Power Transmission: Historical Milestones and System Components," *Proceedings of the IEEE*, vol. 101, no. 6, pp. 1379-1396, 2013.
- [2] A. Pacini, A. Costanzo, S. Aldhaher and P. D. Mitcheson, "Load- and Position-Independent Moving MHz WPT System Based on GaN Distributed Current Sources," *IEEE Transactions on Microwave Theory and Techniques*, vol. 65, no. 12, pp. 5367-5376, 2017.
- [3] K. Kawai, N. Takabayashi, T. Toyonaga, K. Suzuki and N. Shinohara, "Development of Rectenna for Estimating Received Power Level Using Second Harmonic Wave," *Wireless Power Week (WPW), Bordeaux, France, 2022*, pp. 175-179.
- [4] H. Zhang and Y. -X. Guo, "Exploiting High-Isolation 2nd-Harmonic Backscatters for Distance-Adaptive Microwave Power Delivery," *International Applied Computational Electromagnetics Society (ACES-China) Symposium, Chengdu, China, 2021*, pp. 1-2.
- [5] Myun-Joo Park and Byungje Lee, "Dual-band, cross coupled branch line coupler," *IEEE Microwave and Wireless Components Letters*, vol. 15, no. 10, pp. 655-657, Oct. 2005.
- [6] S. -B. Liu, T. Ngo and F. -S. Zhang, "Dual-Band Polarization-Independent Rectenna for RF Energy Harvesting," *IEEE MTT-S International Microwave Workshop Series on Advanced Materials and Processes for RF and THz Applications (IMWS-AMP), Suzhou, China, 2020*, pp. 1-3.